Michigan State University
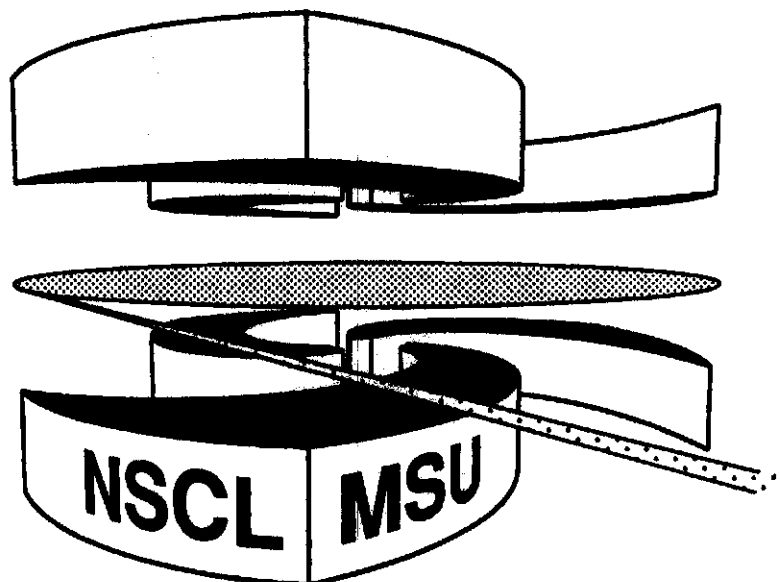
National Superconducting Cyclotron Laboratory

QUADRUPOLE COLLECTIVITY IN ^{32,34,36,38}Si AND THE $N = 20$ SHELL CLOSURE

R.W. IBBOTSON, T. GLASMACHER, B.A. BROWN,
L. CHEN, M.J. CHROMIK, P.D. COTTLE, M. FAUERBACH,
K.W. KEMPER, D.J. MORRISSEY, H. SCHEIT, and
M. THOENNESSEN

Quadrupole collectivity in ^{32,34,36,38}Si and the $N = 20$ shell closure

R.W. Ibbotson[1], T. Glasmacher[1,2], B.A. Brown[1,2], L. Chen[1,2], M.J. Chromik[1*],

P.D. Cottle[3], M. Fauerbach[1,2†], K.W. Kemper[3], D.J. Morrissey[1,4],

H. Scheit[1,2], M. Thoennessen[1,2]

1) National Superconducting Cyclotron Laboratory, Michigan State University,

East Lansing, MI 48824, USA

2) Department Of Physics and Astronomy, Michigan State University,

East Lansing, MI, 48824, USA

3) Department of Physics, Florida State University, Tallahassee, Florida, 32306, USA

4) Department of Chemistry, Michigan State University, East Lansing, MI 48824, USA

(January 16, 1998)

Abstract

The P-unstable nuclei ^{32,34,36,38}Si have been produced by projectile fragmentation and studied by in-beam Coulomb excitation.. Excited states at 1399 $\pm$ 25 keV and 1084 $\pm$ 20 keV have been identified for the first time in ^{36}Si and ^{38}Si, respectively, and tentatively assigned $J^\pi = 2^+$. The $B(E2; 0_1^+ \rightarrow 2_1^+)$ values leading to these states and the previously identified 2_1^+ states in ^{32,34}Si have been measured, and are compared, to shell model calculations. Our results indicate that the 2_1^+ state in ^{34}Si has a large fp-shell intruder component, and that the 2_1^+ states in the N > 20 silicon isotopes can be reproduced assuming an N = 20 shell closure.

The experimental evidence for an "island" of deformed nuclei located near the $N = 20$ shell closure (for $Z < 14$) began to accumulate in 1975 when Thibault et al. [1] found that $^{31}_{11}$Na and $^{32}_{11}$Na are more tightly bound than could be explained with spherical shapes. Since then, data on the energies of levels in the neutron-rich nuclei both in and near this region have been measured. For example, the even-even nuclei ^{36}S and ^{34}Si exhibit high-lying 2^+_1 states (≈ 3 MeV) consistent with these nuclei having an $N = 20$ closed shell and being spherical in their ground-states, while the low-lying 2^+_1 (885 keV) state in the next even-even isotone, $^{32}_{12}$Mg, suggests that this nucleus is strongly deformed. This behavior has been explained by Hartree-Fock [2] and shell-model calculations [3–10] as the filling of neutron $f_{7/2}$ intruder orbits for $Z < 14$ nuclei (i.e., an "inversion" of the standard shell ordering). However, measurements of the $B(E2; 0^+_1 \rightarrow 2^+_1)$ value (hereafter denoted as $B(E2 \uparrow)$) for the neutron-rich nuclei in this "island of inversion" have only recently become possible through the use of Coulomb excitation techniques with radioactive beams. Measurements of $B(E2 \uparrow)$ are much more useful as indicators of collectivity than level energies, since the empirical methods of inferring $B(E2 \uparrow)$ values from the excited-state energies (e.g., [11]) are based on data obtained for nuclei near the valley of stability, and may not apply in the very neutron-rich regions. The $B(E2 \uparrow)$ values inferred from empirical extrapolations are also known to deviate markedly from the measured values for lighter nuclei, especially near closed shells. It is therefore critical to measure these quantities for even-even nuclei in the island of inversion and around its boundary.

Motobayashi et al. [12] determined that in $^{32}_{12}$Mg, which is inside the island of inversion, $B(E2 \uparrow) = 454\pm78$ e^{2}fm^4, corresponding to a deformation parameter[1] of $\beta_2 \approx 0.52$. This rapid change in structure has been interpreted as evidence that the $N = 20$ shell closure

---

[1]If interpreted as a rotational excitation of a statically deformed nucleus, the reduced quadrupole deformation β_2 is related to the $B(E2 \uparrow)$ value by $\beta_2 = \frac{4\pi}{3}\sqrt{B(E2 \uparrow)}/ZeR^2$, neglecting higher-order terms in β_2.

that is so strong in β-stable nuclei is not important for ^{32}Mg. In the present letter, we report the results of a measurement of $B(E2\uparrow)$ values (and excitation energies of the 2_1^+ states) in ^{32,34,36,38}Si using the technique of intermediate-energy Coulomb excitation of beams of these radioactive nuclei and examine the role of fp-shell intruder states in these nuclei.

The ^{32}Si fragments were produced by fragmentation of an 80 MeV/A beam of ^{40}Ar ions provided by the K1200 cyclotron at the NSCL at Michigan State University in a 356 mg/cm^2 ^{9}Be target, separated using a 233 mg/cm^2 ^{27}Al achromatic wedge, and identified at the focal plane of the A1200 fragment separator [13]. The resulting beam was $\approx$ 50% ^{32}Si (at a rate of 15,000/s), with beam contaminants of ^{35}P and ^{40}Ar (8,000/s). These three nuclei were identified at the experimental station on an event-by-event basis by combining the time-of-flight from the end of the A1200 with the energy-loss signal from a thin scintillator. The ^{40}Ar data were analyzed to determine the $E(2_1^+)$ and $B(E2\uparrow)$ in the same manner as the silicon data, as the observed agreement with the well-known values in ^{40}Ar [14] provided a confirmation of the method. The ^{34}Si fragments were produced at a rate of 20,000/s in a separate experiment using the same primary beam/target/wedge combination and a retuning of the A1200. Finally, the ^{36,38}Si nuclei were produced (at 400/s and 50/s, respectively) by fragmentation of a beam of 70 MeV/A ^{48}Ca in a target of 285 mg/cm^2 ^{9}Be, and separated by a thin (5 mg/cm^2) plastic wedge.

The silicon beams were transported from the A1200 to the experimental station and reacted with a gold target. Scattered beam particles were detected in a fast/slow plastic phoswich detector in coincidence with γ rays. The scattering angle for these particles was restricted to be less than 3.8° by the angular extent of the phoswich detector used to identify the fragments. This acceptance defines a minimum distance of closest approach between projectile and target that corresponds to 4 fm greater than the sum of the nuclear radii (assuming R=1.25A$^{1/3}$ fm). This ensures that Coulomb excitation is the dominant excitation process.

An array of 39 cylindrical NaI(Tl) detectors was used for γ ray detection. The array surrounded the target and was completely enclosed in a 16.5 cm thick shielding wall of

low-background lead. The NaI(Tl) crystals were 19 cm long (5.8 cm diameter), with one phototube on each end of the crystal so that the position of the incident γ rays could be determined with approximately 2 cm resolution by light division. This position information allows for Doppler correction of the γ rays on an event-by-event basis. Thinner ^{197}Au targets were used for the ^{32}Si, ^{34}Si and ^{40}Ar experiments (see table I) in order to minimize Doppler broadening due to slowing-down in the target, whereas thicker targets were used for ^{36}Si and ^{38}Si in order to maximize the γ-ray yield. The energy and efficiency calibrations of each NaI detector were determined for a range of energies between 344 keV and 2.614 MeV using standard ^{152}Eu, ^{22}Na, ^{88}Y, ^{60}Co, and ^{228}Th sources. Numerical calculations using GEANT [15] were used to extrapolate this efficiency function to 3.3 MeV using a functional form $\epsilon = \exp\left(a_0 + a_1 \log\left(E_\gamma/E_0\right)\right)$ where E_0 is an arbitrary reference energy and a_0 and a_1 are fitted parameters.

Time-gated γ-ray spectra obtained with ^{32}Si, ^{34}Si, ^{36}Si and ^{38}Si scattered particles are shown in Figure 1. A Doppler correction to the energy of each coincident γ ray was applied on an event-by-event basis. The widths of the observed γ-ray peaks are reduced considerably as a result of the Doppler correction, demonstrating that these γ rays originate in the projectile rest frame, see e.g. [16]. For the scattering angles considered, the ^{197}Au nucleus recoils with ≤ 3 MeV near $90°$ in the laboratory frame; the 547 keV $7/2^+ \rightarrow 3/2^+$ γ ray is therefore artificially broadened in the Doppler-corrected spectra.

Since the excitation probability as well as the efficiency of the NaI array is smaller for the high energy $2_1^+ \rightarrow 0_1^+$ transition in ^{34}Si than for the other transitions studied, a considerably larger amount of data was taken for this nucleus. Notice that the 1.01 MeV γ ray in ^{33}Si, corresponding to 1-neutron removal by the ^{197}Au target, is clearly seen in the spectrum. A weaker 2 MeV γ ray is also seen, possibly corresponding to the 2-n removal channel. This identification could not be verified using the particle information measured with the phoswich detector.

The measured energies of the observed transitions are presented in Table I. The quoted errors include contributions from uncertainties in the Doppler-correction and in the energy

calibration. The agreement of the γ-ray energies from ^{32}Si, ^{34}Si and ^{40}Ar with the known energies demonstrates the correctness of the Doppler shift procedure. While the present data do not allow rigorous J^π assignments for the excited states observed in ^{36,38}Si, we suggest $J^\pi = 2^+$ assignments on the basis of the behavior of nearby even-even nuclei [14].

The extraction of $B(E2 \uparrow)$ values from the measured γ-ray peak areas was performed following the theory of Winther and Alder [17] and was based on a calculation of the excitation probability in first-order perturbation theory. Since the excitation probability of the 2_1^+ state in the present work is $\leq 10^{-4}$ in all cases, this method should be accurate. The two largest contributions to the quoted uncertainties are the statistical uncertainties (in peak size versus background) and the uncertainties in the efficiency.

The reliability of the present measurements of $B(E2 \uparrow)$ is supported by the excellent agreement between the present result for ^{40}Ar ($B(E2 \uparrow) = 372\pm68$ e^{2}fm^4) and the adopted value [18] of 380 ± 14 e^{2}fm^4. The previously determined values for $B(E2 \uparrow)$ in ^{32}Si (by Doppler Shift Attenuation Method measurements of the mean lifetime) are 160 ± 60 e^{2}fm^4 [19] and 308 ± 45 e^{2}fm^4 [20]. The present value for ^{32}Si, $B(E2 \uparrow) = 113\pm33$ e^{2}fm^4, agrees with the former measurement.

The systematic behavior of the $B(E2 \uparrow)$ values in the silicon isotopes (shown with the excitation energies in Figure 2) provides a clearer illustration of the structural evolution than the excitation energies alone. As the neutron number increases from $N = 12$ (^{26}Si), the degree of collectivity smoothly and monotonically decreases until the closed shell is reached at $N = 20$. The collectivity then returns as neutrons are added to the $N = 20$ closed shell, consistent with the assumption that the $N = 20$ shell closure is important in determining the properties of the silicon isotopes. The discrepancy between the measured $B(E2 \uparrow)$ for the proton-rich ^{26}Si [21] and the shell-model prediction discussed below is not presently understood. However, a large experimental disagreement between the measurement of Reference [21] (shown in Figure 2) and a measurement of the relative B(E2) values in the mirror nuclei ^{26}Mg and ^{26}Si from pion scattering [22] suggests that a new measurement of the B(E2) value in ^{26}Si may prove useful.

5

The deformation parameters β_2 extracted from the known $B(E2\uparrow)$ values in the $N = 20$ nuclei, including the present ^{34}Si measurement, are shown in Figure 3. The 2_1^+ states of ^{34}Si, ^{36}S, ^{38}Ar and ^{40}Ca appear to have similar, non-collective structures despite the considerable variation in excitation energies. A very sharp shape change occurs in ^{32}Mg, as the fp-shell intruder state becomes more favored than the $(sd)^{12}$ state. Empirical shell-model calculations have been performed which corroborate this interpretation. In these calculations, we used the same sd-pf Hamiltonian and model space that was used in [16,23] for the neutron-rich S and Ar isotopes. For the $N \neq 20$ silicon isotopes, no neutron excitations were allowed from the sd-shell to the fp-shell. For the $N = 20$ nuclei, however, two separate calculations were performed. In the first, no neutrons were allowed to be excited from the closed $N = 20$ $(sd)^{12}$ ($0\hbar\omega$) configuration. The effective charges used were $e_p = 1.35$ and $e_n = 0.35$. In the second calculation (for the $N = 20$ cases), however, we allowed for the 2p-2h ($2\hbar\omega$) neutron excitations which are responsible for the intruder state in ^{32}Mg. In addition to $(sd)^{12}$ ($0\hbar\omega$) we incorporated the $(d_{5/2})^6$ $(d_{3/2},s_{1/2})^4$ $(f_{7/2},p_{3/2})^2$ ($2\hbar\omega$) configurations. The fp shell restriction to $f_{7/2}$ and $p_{3/2}$ was the same as that assumed in [16,23]. We also restricted the configuration to $(d_{5/2})^6$ in order to keep the matrix dimensions within reasonable limits (less than 5000) as the $d_{5/2}$ orbit is rather deeply bound and its excitation should not be too important. The configurations allowed for the protons were $(d_{5/2})^{n-m}$ $(s_{1/2},d_{3/2})^m$ for ^{30}Ne (n=2), ^{32}Mg (n=4), and ^{34}Si (n=6) with m=0 or 1. For ^{36}S the proton configuration was $(d_{5/2})^{(6-m)}$ $(s_{1/2},d_{3/2})^{(2+m)}$. For the 0+$2\hbar\omega$ calculations and the N>20 $0\hbar\omega$ calculations, the effective charges used were $e_p = 1.35$ and $e_n = 0.65$.

The low-lying spectra for ^{30}Ne, ^{32}Mg, ^{34}Si, ^{36}S and ^{38}Ar obtained with the inclusion of $2\hbar\omega$ configurations are all still dominated by the $0\hbar\omega$ component. In order to reproduce the positions of the intruder states in ^{34}Si and ^{32}Mg the $2\hbar\omega$ components have to be lowered in energy by 8 MeV relative to the $0\hbar\omega$ components. This shift is due to two effects: first, the $2\hbar\omega$ mixture into the $0\hbar\omega$ states tends to push down the energy of the states which are predominantly $0\hbar\omega$. The push comes from the high lying $2\hbar\omega$ states and is very similar to the situation found in a study of ^{16}O in the p-sd model space [24]. The inclusion of $4\hbar\omega$

components which are absent from our model would likewise push down the lowest $2\hbar\omega$ states. Second, the truncations which we have introduced will make the energies of the most collective $2\hbar\omega$ states somewhat smaller than they would be in a more complete model space. A diagonal 8 MeV shift was therefore applied to all $2\hbar\omega$ states. The energies of the lowest calculated 0^+ and 2^+ states are given in Table II. For the $B(E2\uparrow)$ values we have used the same effective charge as in [23].

The results of these calculations for E(2^+) and $B(E2\uparrow)$ are compared to the data for ^{32}Mg, ^{34}Si, ^{36}S, and ^{38}Ar in Figure 3. The $0\hbar\omega$ calculations yield an E(2^+) that is much too high in ^{34}Si, and the $B(E2\uparrow)$ values for ^{32}Mg and ^{34}Si are predicted to be nearly equal, while the experimental results differ by a factor of five. The inclusion of the $2\hbar\omega$ excitations reproduces the dramatic difference in $B(E2\uparrow)$ values between ^{32}Mg and ^{34}Si, as well as predicting the existence of a 2^+ state from the deformed configuration at 2.8 MeV, near the observed 2_1^+ state at 3.328 MeV for ^{34}Si. In order to estimate the effects of $2\hbar\omega$ configurations on the ^{32}Si and ^{36}Si results, the energies of the lowest 2^+ state belonging to the $2\hbar\omega$ configuration have been calculated in the weak-coupling model for ^{32}Si, ^{36}Si and ^{36}S. The $2^+(2\hbar\omega)$ energies for all three cases are 2–3 MeV higher than the $0\hbar\omega$ 2^+ states in these nuclei. Since the inclusion of $2\hbar\omega$ excitations for ^{36}S has little influence on the calculated B(E2) value, the inclusion of such excitations should also have little influence on the ^{32}Si and ^{36}Si calculations. The dramatic effect on the calculated B(E2) values for ^{34}Si and ^{32}Mg occurs because the $2\hbar\omega$ 2^+ state lies energetically below the $0\hbar\omega$ 2^+ state.

The effect of the $2\hbar\omega$ components can be seen in Table 2. The structure of ^{34}Si is predicted from these calculations to be intermediate between that of ^{36}S and ^{32}Mg. While the ground-state in ^{34}Si is still dominated by the "normal" $0\hbar\omega$ configuration (as is ^{36}S), the 2_1^+ state corresponds to the intruder ($2\hbar\omega$) configuration (as in ^{32}Mg). The small $B(E2\uparrow)$ value connecting these states is due to the small overlap of these two wavefunctions. The 2^+ state which corresponds predominantly to the $0\hbar\omega$ configuration is predicted by the current calculations to lie at 4.9 MeV in ^{34}Si (2.8 MeV in ^{32}Mg), which may correspond to the 5.33 MeV state identified in ^{34}Si in Reference [25], that was not observed in [26]. There is

no evidence for a γ ray above 4 MeV corresponding to the decay of such a state in the ^{34}Si spectrum (Figure 1). Experimentally, this places a limit of $B(E2; 0_1^+ \rightarrow 2^+, 5.3 \text{ MeV}) \leq 104 \text{ } e^2\text{fm}^4$ (95% confidence level) on such a transition in ^{34}Si, and the current shell-model calculation predicts a similar value $B(E2; 0_{gs}^+ \rightarrow 2_3^+) = 108 \text{ } e^2\text{fm}^4$.

The present calculations also suggest the existence of a 0_2^+ state (belonging to the intruder configuration, also predicted by [27]) at 2.02 MeV in ^{34}Si, that is linked to the 2_1^+ state by a large $B(E2 \uparrow) = 215 \text{ } e^2\text{fm}^4$. No evidence of a γ ray at 1.3 MeV can be seen in Figure 1. However, this absence does not preclude the existence of a 0^+ state below the 3.328 MeV state as the E_γ^5 dependence of the E2 transition probability function would still strongly favor the transition to the ground state. An E2 transition with the predicted $B(E2; 0_2^+ \rightarrow 2_1^+)$ value (215 $e^2\text{fm}^4$) and a 1.3 MeV decay energy would result in a γ-ray branch with only 2.4% of the intensity of the observed $2_1^+ \rightarrow 0_1^+$ branch, a value that is too weak to be observed in the present experiment or to significantly affect the result of our $B(E2; 0_1^+ \rightarrow 2_1^+)$ measurement.

We have attributed the weak 2.0 MeV γ ray evident in Figure 1 to the 2-neutron removal channel, leading to ^{32}Si. It is possible that this γ ray may actually correspond in whole or in part to the $2_1^+ \rightarrow 0_2^+$ transition. The $B(E2; 0_2^+ \rightarrow 2_1^+)$ value necessary to produce such a branch (assuming that it is entirely $2_1^+ \rightarrow 0_2^+$) is 282 $e^2\text{fm}^4$. The effect of such a branch on the calculation of the $B(E2; 0_1^+ \rightarrow 2_1^+)$ value is within the quoted errors.

In summary, we have measured the $B(E2; 0_1^+ \rightarrow 2_1^+)$ values for ^{32,34,36,38}Si and ^{40}Ar by in-beam Coulomb excitation. The measured energies (for ^{32}Si, ^{34}Si and ^{40}Ar) and $B(E2 \uparrow)$ value (for ^{40}Ar) agree well with previous measurements. This first experimental determination of the degree of quadrupole collectivity in ^{34}Si provides a new experimental boundary on the island of inversion which includes ^{32}Mg. A consistent description of the excitation energy of the 2_1^+ state in ^{34}Si and the $B(E2 \uparrow)$ value is possible in a shell-model space that allows for a large component of the neutron fp-shell ($2\hbar\omega$) intruder state while the ground state corresponds to a $(sd)^{12}$ ($0\hbar\omega$) configuration. The lowest non-intruder 2^+ state is expected to lie at ≈ 4.9 MeV. The measured $B(E2 \uparrow)$ values for the $N > 20$ silicon isotopes can be reproduced assuming an $N = 20$ shell closure for $Z = 14$.

REFERENCES

* Present Address: Ludwig Maximilians Universität München, D-85748 Garching, Germany.

† Present Address: Department of Physics, Florida State University, Tallahassee, FL 32306, USA.

[1] C. Thibault et al., Phys. Rev. **C12** 644 (1975).

[2] X. Campi, H. Flocard, A.K. Kerman and S. Koonin, Nucl. Phys. **A251** 193 (1975).

[3] P. Baumann et al., Phys. Lett. **228B**, 458 (1989).

[4] B.H. Wildenthal and W. Chung, Phys. Rev. **C22** 2260 (1980).

[5] A. Watt, R.P. Singhal, M.H. Storm and R. R. Whitehead, J. Phys. **G7** L145 (1981).

[6] T. Otsuka and N. Fukunishi, Physics Reports **264** 297 (1996).

[7] E.K. Warburton and J.A. Becker, Phys. Rev. **C37** 754 (1988).

[8] E.K. Warburton, J.A. Becker and B.A. Brown, Phys. Rev. **C41** 1147 (1990).

[9] B.A. Brown E.K. Warburton and B.H. Wildenthal, *Exotic Nuclear Spectroscopy*, Plenum Press, NY, 1990 p. 295.

[10] A. Poves and J. Retamosa, Phys. Lett. **184B** 311 (1987).

[11] S. Raman et al., Phys. Rev. **C43** 556 (1991).

[12] T. Motobayashi et al., Phys. Lett. **B346** 9 (1995).

[13] B.M. Sherrill et al., Nucl. Instr. Meth. **B56** 1106 (1991).

[14] P.M. Endt, Nucl. Phys. **A521** 1 (1990).

[15] Computer code GEANT (Version 3.21), unpublished.

[16] H. Scheit et al., Phys. Rev. Lett. **77** 3967 (1996).

[17] A. Winther and K. Alder, Nucl. Phys. **A319** 518 (1979).

[18] P.M. Endt, At. Data. Nucl. Data Tables **23** 3 (1979).

[19] J.G. Pronko and R.E. McDonald, Phys. Rev. **C6** 2065 (1972).

[20] G. Guillaume et al., Nucl. Phys. **A227** 284 (1974).

[21] T.K. Alexander et al., Phys. Lett. **113B** 132 (1982).

[22] C.A. Wiedner et al., Phys. Lett. **97B** 37 (1980).

[23] T. Glasmacher et al., Phys. Lett. **395B** 163 (1997).

[24] E.K. Warburton, B.A. Brown and D.J. Millener, Phys. Lett. **B293** 7 (1992).

[25] L.K. Fifield et al., Nucl. Phys. **A440** 531 (1985).

[26] W.A. Mayer et al., Z. Phys. **A319** 287 (1984).

[27] K. Heyde and J.L. Wood, J. Phys. **G17** 135 (1991).

Nucleus	E_{beam} (MeV/A)	d_{targ} (mg/cm^2)	E(2_1^+) (keV) this work	$\sigma(2_1^+)$ (mb)	$B(E2 \uparrow)$ (e^{2}fm^4)
^{32}Si	37.4	184	1930 (31)	22.1 (64)	113 (33)
^{34}Si	42.6	255	3305 (55)	18.5 (72)	85 (33)
^{36}Si	48.2	532	1399 (25)	67 (21)	193 (59)
^{38}Si	42.2	532	1084 (20)	65 (24)	193 (71)
^{40}Ar	38.4	184	1465 (24)	75.0 (136)	372 (68)

TABLE I. Energies of the first-excited states, excitation cross-sections and $B(E2 \uparrow)$ values leading to these states as determined in the present work. The adopted values of E(2_1^+) for ^{32}Si, ^{34}Si and ^{40}Ar are 1941.5 (2), 3327.7 (5) and 1460.589 (5) keV, respectively [14]. The cross-sections are integrated over $\theta_{lab} < 3.8°$. The incident beam energies E_{beam} include energy-loss due to half the listed target thickness d_{targ}.

	Energies in MeV				$0\hbar\omega$ component (in %)					$B(E2 \uparrow)$ (e^{2}fm^4)
	0_2^+	2_1^+	2_2^+	2_3^+	0_1^+	0_2^+	2_1^+	2_2^+	2_3^+	
^{38}Ar	2.59	1.74	3.34	4.00	86.0	5.8	87.1	6.1	81.5	136
^{36}S	2.52	2.62	3.50	4.20	83.6	9.5	61.7	16.6	8.1	115
^{34}Si	2.02	2.81	4.55	4.94	72.2	14.4	0.4	2.5	63.4	44
^{32}Mg	2.79	0.90	2.26	3.17	4.7	68.8	2.3	1.5	10.6	419
^{30}Ne	3.48	0.89	2.24	3.48	2.9	45.1	1.1	0.2	7.8	337

TABLE II. Excitation energies and $0\hbar\omega$ components of the lowest 0^+ and 2^+ states as calculated by the shell-model technique discussed in the text. The calculated $B(E2; 0_1^+ \to 2_1^+)$ value for each nucleus is also given.

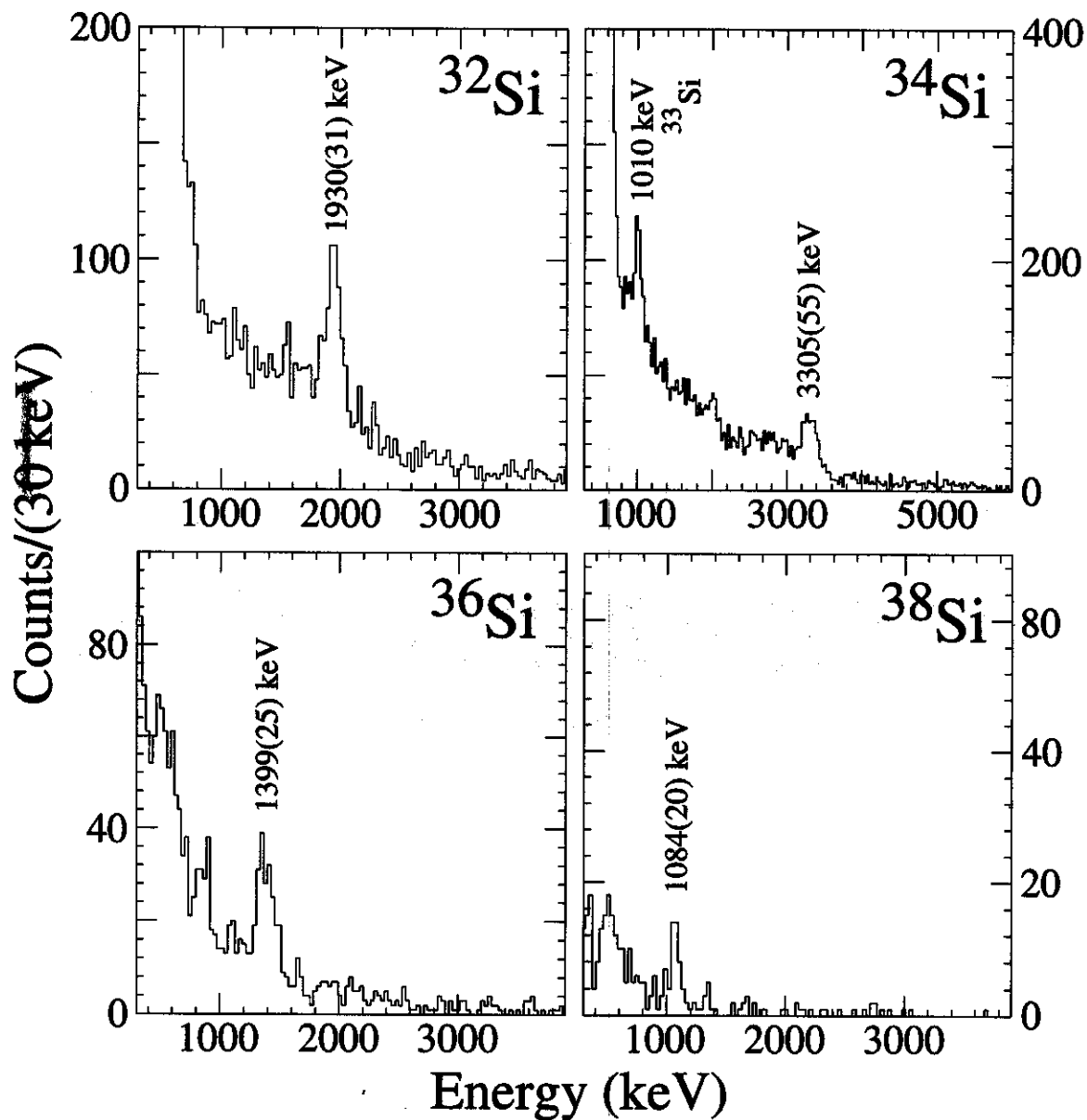FIG. 1. Doppler-corrected γ-ray spectra in coincidence with scattered ^{32}Si, ^{34}Si, ^{36}Si and ^{38}Si particles.
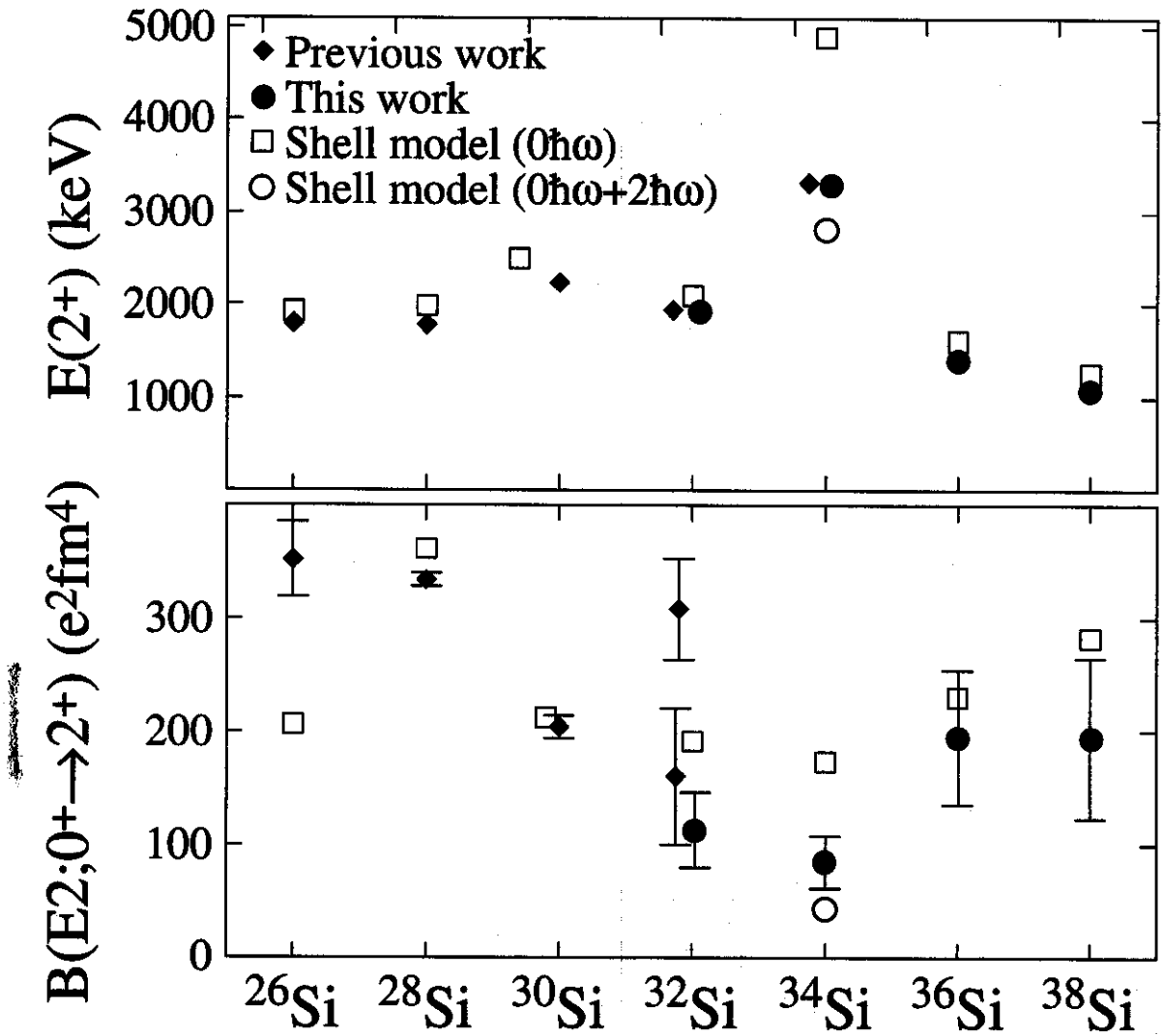
FIG. 2. Measured γ-ray energies and $B(E2; 0^+ \to 2^+)$ values determined in the present work. Previous measurements from [14] are shown in the cases for which they are available. The ^{26}Si, ^{28}Si and ^{30}Si known values are plotted to more fully depict the trends. The shell-model calculations are discussed in the text.
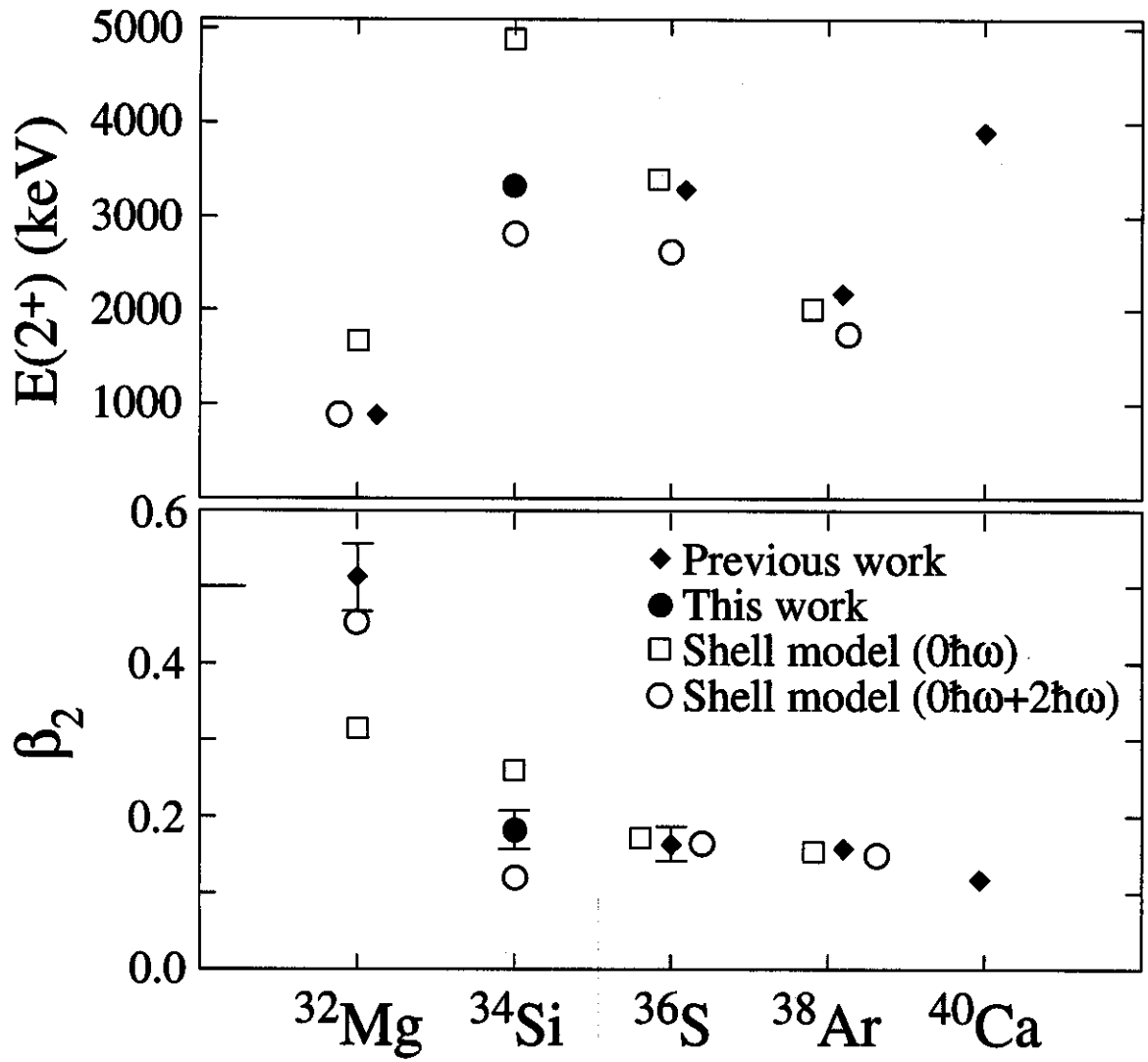
FIG. 3. The deformation parameter β_2 extracted from the known $B(E2\uparrow)$ values in the $N = 20$ nuclei. The ^{34}Si measurement is from the present work.